Slow Timescale Adaptive Control for Multiple-Timescale Systems

Kameron Eves* and John Valasek†
Texas A&M University, College Station, Texas 77843-3141

https://doi.org/10.2514/1.G007439

Multiple-timescale systems are a noteworthy class of dynamic systems that can be modeled with singularly perturbed differential equations. Adaptive control has not been studied in the context of singularly perturbed plants. This paper introduces and evaluates three methods of adaptive control for multiple-timescale systems. Each method is a framework that is valid for a wide class of adaptive control methods. Full-order adaptive control (FOAC) applies adaptive control to the system as a whole. It is straightforward but can be sensitive to timescale effects. Reduced-order adaptive control (ROAC) applies adaptive control to either the fast or slow modes only. This simplifies synthesis but can also constrain the range of valid timescale separation. [K]Control of Adaptive Multiple-Timescale Systems (KAMS) fuses two adaptive control signals using multiple-timescale techniques. KAMS takes advantage of model reduction unlike FOAC, and allows for unstable fast dynamics unlike ROAC. Generalized formal definitions, stability criteria, and examples are developed and presented for each method. Results presented in the paper for the control of a Boeing 747-100/200 on approach show that KAMS has a desirable blend of performance and robustness because each reduced-order model is stabilized separately.

Nomenclature

A_m = slow reference model state matrix
A_x = uncertain slow dynamics state matrix
A_z = fast dynamics state matrix
B_m = slow reference model input matrix
B_x = slow dynamics input matrix
B_z = fast dynamics input matrix
C_m = fast reference model state matrix
d = arbitrary number between zero and one
e_x = error between the slow states and their reference model $x - x_m$
e_z = error between the fast states and their reference model $z - z_m$
e_α = error between the angle of attack and its reference model $\alpha - \alpha_m$
f = function describing the slow time derivative of the slow states
g = function describing the slow time derivative of the fast states
h = function describing the manifold z_0
I = identity matrix
i = integer index
j = integer index
K_r = control gain multiplied by r
$\tilde{K}_r$ = error between the estimate of K_r and its true value $\hat{K}_r - K_r$
K_x = control gain multiplied by x
$\tilde{K}_x$ = error between the estimate of K_x and its true value $\hat{K}_x - K_x$
K_z = control gain multiplied by z
$\tilde{K}_z$ = error between the estimate of K_z and its true value $\hat{K}_z - K_z$
k = function describing the input
L_∞ = set of all functions with bounded L-infinity norms
l = function describing the slow time derivative of the estimate of the uncertain parameters
m = function describing the slow time derivative of the slow reference model states
n = function describing the slow time derivative of the slow reference model input
n_r = number of slow reference model inputs
n_u = number of inputs
n_x = number of slow states
n_z = number of fast states
n_θ = number of uncertain parameters
P_x = solution to the Lyapunov equation for the reference model
P_z = solution to the Lyapunov equation for the closed-loop fast subsystem
p = function describing the slow time derivative of χ
Q_x = arbitrary positive definite matrix
Q_z = arbitrary positive definite matrix
q = body axis pitch rate
q_s = function describing the true value of the slow uncertain parameters θ_s
r = slow reference model input
s = Laplace variable
t = time (arbitrary timescale)
t_f = fast timescale
t_s = slow timescale
t^* = time after which the slow subsystem is a good approximation of the full-order system
u = plant input
u_f = fast input designed to stabilize the fast subsystem
u_s = slow input designed to stabilize the slow subsystem
u = plant input
V = Lyapunov function for the full-order system
V_f = Lyapunov function for the fast subsystem
V_s = Lyapunov function for the slow subsystem
x = plant slow states
x_m = slow reference model states
y = system output
z = plant fast states
z_m = fast reference model states
z_0 = fast state manifold
$\tilde{z}$ = error between the fast states and their manifold $z - z_0$
$\tilde{z}_m$ = error between the fast states reference model and the manifold $z_m - z_0$
α = angle of attack

Presented as Paper 2023-1444 at the AIAA SciTech Forum and Exposition, National Harbor, MD, January 23–27, 2023; received 20 December 2022; revision received 29 May 2023; accepted for publication 12 June 2023; published online 4 August 2023.

*Graduate Research Assistant, Vehicle Systems & Control Laboratory, Aerospace Engineering Department; currently Assistant Professor, Electrical & Computer Engineering, Utah Tech University; Kameron.Eves@utahtech.edu. Member AIAA.

†Professor and Director, Vehicle Systems & Control Laboratory, Aerospace Engineering Department; valasek@tamu.edu. Fellow AIAA.

α_i = real numbers that are derived from the Lyapunov functions of the subsystems $i \in \{1, 2\}$
β_i = real numbers that are derived from the Lyapunov functions of the subsystems $i \in \{1, 2\}$
Γ_r = adaptation rate gain for $\hat{K}_r$
Γ_x = adaptation rate gain for $\hat{K}_x$
Γ_{xz} = adaptation rate gain for $\hat{K}_x$ and $\hat{K}_z$
γ = real number that is derived from the Lyapunov functions of the subsystems
δ_e = elevator deflection
$\delta_{e,c}$ = commanded elevator deflection
$\delta_{e,c,f}$ = equivalent to u_f but specifically referring to commanded elevator deflection
$\delta_{e,c,s}$ = equivalent to u_s but specifically referring to commanded elevator deflection
$\delta_{e,0}$ = elevator deflection manifold
ϵ = timescale separation parameter $\epsilon \triangleq t_s/t_f$
ϵ^* = supremum for the timescale separation parameter
θ = uncertain parameters
θ_f = uncertain parameters in the fast subsystem
θ_s = uncertain parameters in the slow subsystem
$\tilde{\theta}$ = error between the estimates of the uncertain parameters and their true value $\hat{\theta} - \theta$
Λ = uncertain positive definite control effectiveness matrix
$\lambda_{\min}(\cdot)$ = smallest eigenvalue of $(\cdot)$
$\sigma_{\max}(\cdot)$ = maximum singular value of $(\cdot)$
Φ = arbitrary function of e_x used to show stability
χ = several states concatenated together $[\boldsymbol{x}^T \ \hat{\boldsymbol{\theta}}^T \ \boldsymbol{x}_m^T \ \boldsymbol{r}^T]^T$
Ψ = arbitrary function of $\tilde{z}$ used to show stability
$(\dot{\cdot})$ = time derivative with respect to the fast timescale $d(\cdot)/dt_f$
$(\acute{\cdot})$ = time derivative with respect to the slow timescale $d(\cdot)/dt_s$
$\hat{(\cdot)}$ = estimate of $(\cdot)$
$\|(\cdot)\|_2$ = L-2 norm of $(\cdot)$
$0_{i\times j}$ = $i \times j$-dimensional matrix of zeros

I. Introduction

MANY dynamic systems can be modeled as multiple-timescale systems using singular perturbation theory. Most systems with fast and slow modes are good candidates for this type of modeling. Linear systems meet this criterion when they have two or more natural frequencies that differ by an order of magnitude. However, multiple-timescale control can be applied to nonlinear systems too [1]. Multiple-timescale models have been developed for robotic arms [2], electrical circuits [3], and even abstract systems like manufacturing processes [4]. Many systems with actuator dynamics can be modeled as a multiple-timescale system [5]. The separation of the phugoid and short-period mode make fixed-wing aircraft multiple-timescale systems. Multiple-timescale models have been published for F-16 aircraft [6] and hypersonic aircraft [7]. Several examples of multiple-timescale models for aerospace systems are given in [8], including digital flight control systems, atmospheric entry, satellites, interplanetary trajectories, missiles, launch vehicles, hypersonic flight, orbital transfers, flexible aerospace structures, and space robotics. Despite their omnipresence, the vast majority of multiple-timescale control research focuses on systems with known and time-invariant system models. Adaptive control directly addresses systems with unknown and time-varying system models. However, the effect of singularly perturbed plants on adaptive control is yet to be fully explored. This paper addresses this gap in the literature by investigating the benefits, complexities, and limitations of adaptive control for multiple-timescale systems.

In this paper, singular perturbation theory is used to model and analyze multiple-timescale behavior in the system plant. However, some adaptive control researchers have applied singular perturbation theory to control equations. Hovakimyan et al. developed such a technique that numerically converges to dynamic inversion [9]. This is useful for algebraically intractable systems. Lavretsky and Hovakimyan then expanded this method to explicitly include adaptive control methods [10]. Hovakimyan and Lavretsky used singular perturbation to ensure that the numerical convergence of the control occurred faster than the dynamics of the system. Sun et al. used a similar technique on underactuated Euler–Lagrange systems [11]. Krishnamurthy and Khorrami investigated a similar technique for a class of systems with nonlinear input uncertainty [12]. Asadi and Khayatiyan [13] as well as Chakrabortty and Arcak [14] both examined a similar technique on a class of systems with matched and unmatched uncertainty. Finally, Rayguru et al. [15] and Yang et al. [16] showed a similar technique's applicability to systems with input saturation. Each of these examples used singular perturbation in the *control architecture*. This paper addresses systems with *plants* that are singularly perturbed.

Prior research into adaptive control for singularly perturbed plants falls into two broad categories. These categories are identified for the first time here and will be called reduced-order adaptive control (ROAC) and full-order adaptive control (FOAC). ROAC separates the fast and slow dynamics and then only applies adaptive control to one of the two. FOAC applies adaptive control to the full-order system. Examples of ROAC include Al-Radhawi et al., who modeled the COVID-19 pandemic as a multiple-timescale system with adaptive control applied to the fast subsystem [17]; Macchelli et al., who modeled a leaking hydraulic press as a multiple-timescale system and showed that the slow timescale leaking did not affect the adaptive control in the fast timescale [18]; and Nguyen et al., who applied adaptive control to an aircraft's pitch dynamics when the elevator is on a timescale that is much slower than the pitch dynamics [5]. Saha et al. demonstrated a form of FOAC. They expanded sequential multiple-timescale control to systems with model uncertainty. This was applied to an F-16 aircraft [6,19], a spring-mass-damper [20], and a satellite [21]. To do so, Saha et al. used parameter estimators from adaptive control literature, but they did not use traditional adaptive *control* techniques. That being said, Saha et al.'s method is, in fact, a type of multiple-timescale adaptive control because the adaptive parameters are used in the control.

As described above, prior works in the literature on ROAC and FOAC have not been formalized and used only for specific systems. In the present work they are formalized and generalized to a wide class of plants for the first time. More significantly, this work introduces and develops a novel method of adaptive control for multiple-timescale systems called [K]Control of Adaptive Multiple-Timescale Systems (KAMS). Both ROAC and FOAC use elements of adaptive control and multiple-timescale control. KAMS fully and rigorously merges these two fields using a separate controller for the slow and fast dynamics, and then one of several multiple-timescale control techniques to fuse the two signals together. KAMS is similar to the control proposed by Ioannou and Kokotovic, but more general in that it addresses nonlinear systems and allows for increased coupling [22]. The most general version of KAMS does allow adaptation in both the fast and slow subsystems, but this paper focuses on the prefatory problem of slow state tracking of a reference model with slow timescale adaptation. Specifically, all adaptation is in the slow timescale and the control objective is to stabilize the slow states, but the methods presented are extensible to other cases. Section II introduces the mathematical notation. Section III describes the three adaptive control methodologies for multiple-timescale systems. Section IV shows a numerical example of all three methods on the multiple-timescale pitch rate dynamics of a Boeing 747-100/200 with actuator dynamics. This example highlights the similarities and differences between the three methods showing that all three multiple-timescale adaptive control methodologies are effective, and each method has benefits and detriments.

II. Mathematical Preliminaries

Multiple-timescale systems are typically modeled as a system of singularly perturbed differential equations with the form

$$\acute{\boldsymbol{x}} = f(\boldsymbol{x}, \boldsymbol{z}, \boldsymbol{u}) \tag{1a}$$

$$\epsilon \acute{\boldsymbol{z}} = g(\boldsymbol{x}, \boldsymbol{z}, \boldsymbol{u}, \epsilon) \tag{1b}$$

In this system, $\boldsymbol{u} \in \mathbb{R}^{n_u}$ is the input vector; $\boldsymbol{x} \in \mathbb{R}^{n_x}$ and $\boldsymbol{z} \in \mathbb{R}^{n_z}$ are both system state vectors. The accents above $\boldsymbol{x}$ and $\boldsymbol{z}$ on the left-hand side are time derivatives. The timescale separation parameter $0 < \epsilon \ll 1$ is a very small number. The functions f and g must be of relatively the same order of magnitude so that in general $\dot{\boldsymbol{x}} \ll \acute{\boldsymbol{z}}$. Because of this relationship, $\boldsymbol{x}$ is called the slow states and $\boldsymbol{z}$ is called the fast states. Due to the relative speed difference, it is easier to describe the motion of the fast states using different units for time. These units are called timescales. The subscript s is used to identify when the time is in slow timescale (t_s) and the subscript f is used for the fast timescale (t_f). The timescale separation parameter ϵ is the ratio of the timescales $\epsilon = t_s/t_f$. For example, let $\epsilon = 1/60$. After 1 minute has passed $t_s = 1$ minute and $t_f = 60$ s. The two different timescales allow for two different time derivatives. In this present work, the derivative with respect to the slow timescale is denoted $d(\cdot)/dt_s = \dot{(\cdot)}$ and the derivative with respect to the fast timescale is denoted $d(\cdot)/dt_f = \acute{(\cdot)}$. Using the definition of the timescale separation parameter, it can be seen that $\epsilon\acute{(\cdot)} = \dot{(\cdot)}$. Practically, the timescale separation parameter can be difficult to determine for nonlinear systems, but control techniques exist that do not require precise knowledge of the timescale separation parameter [1].

One common analysis technique for multiple-timescale systems is to approximate the system with two separate asymptotic solutions. Taking the limit of Eq. (1) as $\epsilon \to 0$ gives

$$\acute{\boldsymbol{x}} = f(\boldsymbol{x}, \boldsymbol{z}, \boldsymbol{u}) \tag{2a}$$

$$0 = g(\boldsymbol{x}, \boldsymbol{z}, \boldsymbol{u}, 0) \tag{2b}$$

If Eq. (2b) can be solved for $\boldsymbol{z}$ such that $\boldsymbol{z}_0 = h(\boldsymbol{x}, \boldsymbol{u})$ then the system is called *standard*. The trajectory $\boldsymbol{z}_0$ is called the *fast state manifold* or more simply the *manifold*. Physically, it represents the steady-state trajectory of the fast states. Thus, the first asymptotic model is

$$\acute{\boldsymbol{x}} = f(\boldsymbol{x}, \boldsymbol{z}_0, \boldsymbol{u}) \tag{3a}$$

$$\boldsymbol{z}_0 = h(\boldsymbol{x}, \boldsymbol{u}) \tag{3b}$$

Using the relationship between the slow and fast derivatives $\epsilon\acute{(\cdot)} = \dot{(\cdot)}$, Eq. (1) can be converted to

$$\dot{\boldsymbol{x}} = \epsilon f(\boldsymbol{x}, \boldsymbol{z}, \boldsymbol{u}) \tag{4a}$$

$$\dot{\boldsymbol{z}} = g(\boldsymbol{x}, \boldsymbol{z}, \boldsymbol{u}, \epsilon) \tag{4b}$$

The second asymptotic model is then found by again taking the limit as $\epsilon \to 0$:

$$\dot{\boldsymbol{x}} = 0 \tag{5a}$$

$$\dot{\boldsymbol{z}} = g(\boldsymbol{x}, \boldsymbol{z}, \boldsymbol{u}, 0) \tag{5b}$$

Equations (3) and (5) are called the reduced slow model and the reduced fast model, respectively. Vasil'eva [23] and Tikhonov [24] developed conditions under which the system will be approximated by the reduced subsystems. This is known as Tikhonov's theorem ([25], Theorem 9.1). Conceptually Tikhonov's theorem says that the fast states converge quickly to the manifold after which the slow states evolve according to the reduced slow model. Notably, Tikhonov's theorem requires that the system be standard, but similar results have been found for nonstandard systems using geometric singular perturbation theory [1].

Various control techniques for multiple-timescale systems exist. In this paper composite control will be used. Composite control designs two control signals, one to stabilize the slow states ($\boldsymbol{u}_s(\boldsymbol{x})$) and one to drive the fast states to the manifold ($\boldsymbol{u}_f(\boldsymbol{x}, \boldsymbol{z})$). These two control signals are summed together so that

$$\boldsymbol{u} = \boldsymbol{u}_s(\boldsymbol{x}) + \boldsymbol{u}_f(\boldsymbol{x}, \boldsymbol{z}) \tag{6}$$

Notably, $\boldsymbol{u}_f$ is chosen so that $\boldsymbol{u}_f(\boldsymbol{x}, \boldsymbol{z}_0) = 0$. This requires knowledge of the manifold.

III. Adaptive Control Methodologies

Consider the control objective of slow state tracking of a reference model. The reference model is

$$\acute{\boldsymbol{x}}_m = A_m \boldsymbol{x}_m + B_m \boldsymbol{r} \tag{7}$$

where $A_m \in \mathbb{R}^{n_x \times n_x}$ and $B_m \in \mathbb{R}^{n_x \times n_r}$ are parameters, and $\boldsymbol{r} \in \mathbb{R}^{n_r}$ is the reference model input. For all systems considered herein, the system output is $\boldsymbol{y} = \boldsymbol{x}$. Let $\boldsymbol{\theta} \in \mathbb{R}^{n_\theta}$ be the true value of uncertain parameters and $\hat{\boldsymbol{\theta}}$ be the adaptive estimate of those parameters. If direct adaptive control is used, then these parameters are control gains. If indirect adaptive control is used, then these parameters are system parameters. Note that at this point no precise structure for the control law is given. This is because FOAC, ROAC, and KAMS as described herein are highly generalized and applicable to a wide class of adaptive control methods. At this point any control law that fits the format $\boldsymbol{u} = k(\boldsymbol{x}, \hat{\boldsymbol{\theta}}, \boldsymbol{x}_m, \boldsymbol{r}, \boldsymbol{z})$ is valid. As is any adaptation law that fits the format $\acute{\hat{\boldsymbol{\theta}}} = l(\boldsymbol{x}, \boldsymbol{x}_m)$. Slightly stricter definitions will be given later in this paper as necessary. Three error signals can be defined using the reference model, the manifold, and the parameter estimates. These errors are similar to those seen in traditional adaptive control (e.g., [26]), but the appearance and role of the manifold is a unique aspect of the multiple-timescale adaptive control problem. The error terms are

$$\boldsymbol{e}_x \triangleq \boldsymbol{x} - \boldsymbol{x}_m \tag{8a}$$

$$\tilde{\boldsymbol{z}} \triangleq \boldsymbol{z} - \boldsymbol{z}_0 \tag{8b}$$

$$\tilde{\boldsymbol{\theta}} \triangleq \hat{\boldsymbol{\theta}} - \boldsymbol{\theta} \tag{8c}$$

In a few cases, a reference model is needed for the fast states

$$\dot{\tilde{\boldsymbol{z}}}_m = C_m \tilde{\boldsymbol{z}}_m \tag{9}$$

Another error can be defined as

$$\boldsymbol{e}_z \triangleq \tilde{\boldsymbol{z}} - \tilde{\boldsymbol{z}}_m \tag{10a}$$

$$= \boldsymbol{z} - \boldsymbol{z}_m \tag{10b}$$

where $\boldsymbol{z}_m$ is defined such that the pattern $\tilde{\boldsymbol{z}}_m = \boldsymbol{z}_m - \boldsymbol{z}_0$ holds.

A. Full-Order Adaptive Control

The most intuitive solution to multiple-timescale adaptive control is to treat multiple-timescale systems like other systems. Equation (1) can be rewritten as

$$\acute{\boldsymbol{x}} = f(\boldsymbol{x}, \boldsymbol{z}, \boldsymbol{u}) \tag{11a}$$

$$\acute{\boldsymbol{z}} = \frac{1}{\epsilon} g(\boldsymbol{x}, \boldsymbol{z}, \boldsymbol{u}, \epsilon) \tag{11b}$$

In which $\boldsymbol{x}$ and $\boldsymbol{z}$ can be concatenated into a single state vector. If a valid adaptive control methodology exists for the resulting system, then there is no reason that the adaptive control algorithm will not work. The following theorem formalizes this conceptual definition of FOAC.

Theorem 1: Consider the system in Eq. (1). If there exists an adaptive controller that accomplishes the control objective for the equivalent system in Eq. (11) and assuming that said adaptive control

problem is well-posed (i.e., its assumptions are satisfied), then the adaptive controller for Eq. (11) is also valid for Eq. (1).

Proof: The timescale separation parameter, whereas often unknown, is simply a fixed scalar value. Additionally, the timescale separation parameter is very small, but not zero. Thus, dividing by the timescale separation parameter is valid. Further, dividing by the timescale separation parameter does not affect the time evolution the system states $\boldsymbol{x}$ and $\boldsymbol{z}$. □

Theorem 1 seems simple and obvious, but the results are significant to FOAC. Effectively, Theorem 1 states that the singularly perturbed nature of Eq. (1) does not inhibit the use of normal adaptive control techniques. Theorem 1 seems to imply that multiple-timescale systems are no different from traditional systems and can be controlled similarly. However, Theorem 1 is not always robust to timescale effects. For example, timescale effects can cause high-frequency oscillations. This is demonstrated in the example at the end of this paper. Sensitivity to the timescale separation parameter is a major disadvantage because the timescale separation parameter is frequently unknown. This is particularly true for systems with model uncertainties because the timescale separation parameter is a function of system parameters and is related to the form of the dynamics. In other words, multiple-timescale systems that require adaptive control are even more likely to have large uncertainty bounds on the timescale separation parameter. This problem is exacerbated by the ϵ^{-1} term in Eq. (11). Because $0 < \epsilon \ll 1$, small inaccuracies in estimating the timescale separation parameter can cause large discrepancies between the predicted and actual system response. Traditional multiple-timescale control methodologies account for this problem by giving a range of valid timescale separation parameters. However, Theorem 1 does not immediately give rise to any such valid range.

B. Reduced-Order Adaptive Control

If either the reduced fast model or the reduced slow model is stable, then one intuitive approach to adaptive multiple-timescale control is to apply adaptive control to the other reduced-order model and rely on the inherent stability of the discounted dynamics to assure convergence. This technique is ROAC and is by far the most common method of designing controllers for multiple-timescale systems. All models that discount fast actuator dynamics inherently apply ROAC.

The problems incurred by reducing a model have been studied in the adaptive control literature, in which the discounted dynamics are often treated as a time delay (e.g., [27]) or unmodeled dynamics (e.g., [28]). The primary challenge is that inputs to one reduced-order model can excite dynamic modes in the other reduced-order model. It has been shown that even stable discounted dynamics can be driven unstable in this manner [29]. Narang-Siddarth and Valasek demonstrated this problem with multiple-timescale systems ([1], p. 46).

Theorem 2: Consider the system in Eq. (1), its reduced-order models in Eqs. (3) and (5), and its manifold $\boldsymbol{z}_0$. Suppose that the following conditions are true:

A) Let $\acute{\boldsymbol{x}}_m = m(\boldsymbol{x}_m, \boldsymbol{r})$ be a reference model for the slow states with input $\boldsymbol{r}$.

B) Assume that $\boldsymbol{r}, \acute{\boldsymbol{r}} \in L_\infty$ and $\acute{\boldsymbol{r}} = n(t_s)$.

C) Given a valid adaptive controller, $\boldsymbol{u} = k(\boldsymbol{x}, \hat{\boldsymbol{\theta}}, \boldsymbol{x}_m, \boldsymbol{r})$, which satisfies the control objective for the reduced slow model.

D) Let $\hat{\acute{\boldsymbol{\theta}}} = l(\boldsymbol{x}, \boldsymbol{x}_m)$ be the adaptive laws for that adaptive controller.

E) Assume that the functions f, g, k, l, m, and n are continuous for all $\boldsymbol{x}$, $\boldsymbol{z}$, and t.

F) Also assume that the system is standard such that the manifold exists and the reduced subsystems are well defined.

G) Assume that in the context of the closed-loop full-order dynamics the fast state manifold $\boldsymbol{z}_0$ is an asymptotically stable equilibrium and the initial conditions are within the region of attraction for that equilibrium.

H) Finally, assume that $\hat{\acute{\boldsymbol{\theta}}}$, $\acute{\boldsymbol{x}}_m$, and $\acute{\boldsymbol{r}}$ are on the order of (i.e., have the same order of magnitude as) $\acute{\boldsymbol{x}}$.

Then there exists a timescale separation parameter $0 < \epsilon^* \ll 1$, and ∃ a time after the initial time $t_0 < t^*(\epsilon^*)$ such that $\forall \epsilon < \epsilon^*$ the difference between the closed-loop full-order model, and the closed-loop reduced slow model is on the order of ϵ^* after t^*.

Proof: Consider the full-order closed-loop dynamics. Define a new state vector

$$\boldsymbol{\chi} \triangleq \begin{bmatrix} \boldsymbol{x}^T & \hat{\boldsymbol{\theta}}^T & \boldsymbol{x}_m^T & \boldsymbol{r}^T \end{bmatrix}^T \tag{12}$$

Using the definitions given by (A), (B), and (D),

$$\acute{\boldsymbol{\chi}} = \begin{bmatrix} f(\boldsymbol{x}, \boldsymbol{z}, \boldsymbol{u})^T & l(\boldsymbol{x}, \boldsymbol{x}_m)^T & m(\boldsymbol{x}_m, \boldsymbol{r})^T & n(t)^T \end{bmatrix}^T \tag{13}$$

Recall from (C) that $\boldsymbol{u} = k(\boldsymbol{x}, \hat{\boldsymbol{\theta}}, \boldsymbol{x}_m, \boldsymbol{r})$ and substitute

$$\acute{\boldsymbol{\chi}} = \begin{bmatrix} f(\boldsymbol{x}, \boldsymbol{z}, k(\boldsymbol{x}, \hat{\boldsymbol{\theta}}, \boldsymbol{x}_m, \boldsymbol{r}))^T & l(\boldsymbol{x}, \boldsymbol{x}_m)^T & m(\boldsymbol{x}_m, \boldsymbol{r})^T & n(t)^T \end{bmatrix}^T \tag{14}$$

Let p be a vector function such that

$$\acute{\boldsymbol{\chi}} = p(\boldsymbol{\chi}, \boldsymbol{z}, t) \tag{15}$$

Now recall the full-order closed-loop fast state dynamics $\epsilon \acute{\boldsymbol{z}} = g(\boldsymbol{x}, \boldsymbol{z}, \boldsymbol{u}, \epsilon)$. Similar to $\acute{\boldsymbol{\chi}}$, $\acute{\boldsymbol{z}}$ can be rewritten using (C):

$$\epsilon \acute{\boldsymbol{z}} = g(\boldsymbol{x}, \boldsymbol{z}, k(\boldsymbol{x}, \hat{\boldsymbol{\theta}}, \boldsymbol{x}_m, \boldsymbol{r}), \epsilon) \tag{16}$$

or equivalently

$$\epsilon \acute{\boldsymbol{z}} = g(\boldsymbol{\chi}, \boldsymbol{z}, \epsilon) \tag{17}$$

Due to condition (H), all of the states in χ are of the same timescale. Thus Eqs. (15) and (17) taken together form a multiple-timescale system:

$$\acute{\boldsymbol{\chi}} = p(\boldsymbol{\chi}, \boldsymbol{z}, t) \tag{18a}$$

$$\epsilon \acute{\boldsymbol{z}} = g(\boldsymbol{\chi}, \boldsymbol{z}, \epsilon) \tag{18b}$$

Note that the manifold for this new multiple-timescale system representing the closed-loop dynamics is the same as the manifold for the open-loop dynamics. Due to conditions (E), (F), and (G) Eq. (18) is in the proper format to apply Tikhonov's theorem ([1], Theorem 1). Thus, via Tikhonov's theorem, there exists a timescale separation parameter $0 < \epsilon^* \ll 1$ and ∃ a time after the initial time $t_0 < t^*(\epsilon^*)$ such that $\forall \epsilon < \epsilon^*$ the difference between the closed-loop full-order model and the closed-loop reduced slow model is on the order of ϵ^* after t^*. □

Two corollaries follow directly from Theorem 2:

Corollary 1: If the conditions of Theorem 2 are met and the closed-loop reduced slow system is bounded, then the closed-loop full-order system is also bounded.

Corollary 2: If the conditions of Theorem 2 are met and the reference model is an asymptotically stable equilibrium of the closed-loop reduced slow system with the initial conditions being in the region of attraction for this equilibrium, then after time t^* the error between the reference model and the slow states of the closed-loop full-order system is on the order of the timescale separation. Succinctly the system is stable about the reference model in the sense of Lyapunov.

In a general sense, Theorem 2 and its associated corollaries state that an adaptive controller designed for the reduced slow model also stabilizes the full-order model if the system can be rewritten such that Tikonov's theorem applies. Theorem 2 only applies to systems with adaptive control in the reduced slow system. Applying a similar derivation to adaptive control for the reduced fast model makes the closed-loop system nonstandard, and, as a result, Tikonov's theorem does not apply. However, some researchers have managed to use a similar process to prove boundedness for specific systems with adaptive control on the reduced fast model (e.g., [5]). Generalizing this procedure is the subject of ongoing research.

Notably, Tikhonov's theorem, and by association Theorem 2, implies stability in the sense of Lyapunov, but not convergence. This

is interesting to consider in the common case of discounted actuator dynamics. Recall from Theorem 2 that the bound on the slow state tracking is of the order of the timescale separation parameter. This means that speeding up the actuators (effectively increasing the timescale separation by decreasing the timescale separation parameter) can improve tracking performance. This formalizes the common wisdom that faster actuators are preferable.

There are many conditions in Theorem 2, but the most difficult to satisfy is usually that the closed-loop manifold is an asymptotically stable equilibrium of the fast states [condition (G)]. This gets back to the heart of the problem discussed at the beginning of this section; i.e., controlling a subset of the dynamics can drive the discounted dynamics unstable. Sometimes, a Lyapunov function can be found for the system that proves that the manifold is asymptotically stable (see [26], Theorem 3.4.1 Statment iii). However, valid Lyapunov functions can prove evasive for some systems.

C. [K]Control of Adaptive Multiple-Timescale Systems

ROAC requires that the discounted reduced model be stable. Further, the difficulty of applying ROAC stems from proving that the closed-loop manifold is an asymptotically stable equilibrium of the fast dynamics. If some method could be found to ensure the stability of the discounted dynamics without affecting the primary reduced-order model, it could simplify and expand the applicability of ROAC. For this purpose, KAMS is introduced. KAMS uses multiple-timescale control techniques to control both the reduced fast model and the reduced slow model simultaneously. Herein, composite control will be used. The final control law takes the form of Eq. (6), but some minor alterations are needed to account for the additional adaptive signals:

$$\boldsymbol{u} = \boldsymbol{u}_s(\boldsymbol{x}, \hat{\boldsymbol{\theta}}_s, \boldsymbol{x}_m, \boldsymbol{r}) + \boldsymbol{u}_f(\boldsymbol{x}, \hat{\boldsymbol{\theta}}_s, \boldsymbol{x}_m, \boldsymbol{r}, \tilde{z}) \tag{19}$$

Conceptually, the slow control stabilizes the reduced slow system and the fast control stabilizes the reduced fast system. Thus KAMS requires the design of two individual controllers. Each controller can be adaptive or nonadaptive depending on where the model uncertainties appear in the reduced-order models. If both controllers are selected to be nonadaptive, then the control is reduced to typical composite control. Just like composite control, it is requisite that the fast control be zero when the fast states have reached their manifold. If the fast control is selected to be nonadaptive, then Theorem 2 still applies. Theorem 3 states this logic more formally.

Theorem 3: Let all of the conditions of Theorem 2 be satisfied except condition (C). In place of condition (C), let condition (I) be the control given in Eq. (19), where the slow control $\boldsymbol{u}_s$ is selected to be an adaptive controller with parameters $\hat{\boldsymbol{\theta}}_s$, reference model $\boldsymbol{x}_m$, and reference model input $\boldsymbol{r}$. The fast control is selected to be a nonadaptive control method. Then the conclusions of Theorem 2 and its associated Corollaries 1 and 2 are still valid.

Proof: The only difference between Theorem 2 and Theorem 3 is that the fast states appear in the control $u = k(\boldsymbol{x}, \hat{\boldsymbol{\theta}}_s, \boldsymbol{x}_m, \boldsymbol{r}, \boldsymbol{z})$. The general procedure to prove Theorem 2 is to augment the slow states with the new differential equations, substitute the control into all of the differential equations, and show that the resulting differential equations are still of the form required by Tikhonov's theorem. Because $\boldsymbol{u}_f$ is nonadaptive there are no additional differential equations beyond those discussed in the proof of Theorem 2. Thus it is sufficient to show that the control is only substituted into functions that are already dependent upon the fast states (i.e., adding the fast states to the control did not change the domain of the closed-loop differential equations). Checking Eqs. (14) and (16) it can be seen that this is the case. Therefore, Eq. (18) is still valid. The remainder of the proof follows the proof of Theorem 2. The logic of Corollaries 1 and 2 is not affected. □

Because KAMS specifically designs a controller for the dynamics of both reduced systems, the assumption that one of the two reduced subsystems is inherently stable is relaxed. Another benefit of KAMS is that because the stability of the reduced fast subsystem is asserted instead of assumed, it is easier to prove that the manifold of the closed-loop system is an asymptotically stable equilibrium. In fact, for some forms of nonlinear control, a valid Lyapunov function could be directly implied by the control design. Saberi and Khalil showed a method to find a valid range for the timescale separation parameter under composite control [30]. In some cases, the limits of this range are dependent upon the control gains. Thus, the third benefit of KAMS is that the range of valid timescale separation parameters can be larger (see Sec. IV for an example of this). Saberi and Khalil's technique can be expanded to apply to KAMS. This is generalized with the following theorem. Just like Sec. III.B, only the case of adaptive control in the slow states is considered.

Theorem 4: Assume that all of the conditions of Theorem 3 apply. Add the condition (J) on the true time-varying parameters $\boldsymbol{\theta}_s = q_s(\boldsymbol{x}, t_s)$, where $\boldsymbol{\theta}_s$ evolves on the slow timescale. Let $V_s(\boldsymbol{e}_x, \tilde{\boldsymbol{\theta}}_s)$ and $V_f(\tilde{z})$ be candidate Lyapunov functions. Let $0 < \alpha_1, \alpha_2, \beta_1, \beta_2, \gamma \in \mathbb{R}$ be arbitrary. Let $\Psi(\boldsymbol{e}_x)$ and $\Phi(\tilde{z})$ be arbitrary continuous scalar functions such that $\Psi(0) = \Phi(0) = 0$.

If the following conditions are met,

$$\frac{\partial V_s}{\partial \boldsymbol{e}_x}(f(\boldsymbol{x}, z_0, \boldsymbol{u}_s) - m(\boldsymbol{x}_m, \boldsymbol{r})) + \frac{\partial V_s}{\partial \tilde{\boldsymbol{\theta}}_s}\left(l(\boldsymbol{x}, \boldsymbol{x}_m) - \dot{q}_s(\boldsymbol{x}, t_s)\right) \leq -\alpha_1 \Psi^2(\boldsymbol{e}_x) \tag{20a}$$

$$\frac{\partial V_f}{\partial \tilde{z}}\left(g(\boldsymbol{x}, z, \boldsymbol{u}, 0) - \dot{h}(\boldsymbol{x}, \boldsymbol{u}_s)\right) \leq -\alpha_2 \Phi^2(\tilde{z}) \tag{20b}$$

$$\frac{\partial V_s}{\partial \boldsymbol{e}_x}(f(\boldsymbol{x}, z, \boldsymbol{u}) - f(\boldsymbol{x}, z_0, \boldsymbol{u}_s)) \leq \beta_1 \Psi(\boldsymbol{e}_x)\Phi(\tilde{z}) \tag{20c}$$

$$\frac{\partial V_f}{\partial \tilde{z}}(g(\boldsymbol{x}, z, \boldsymbol{u}, \epsilon) - g(\boldsymbol{x}, z, \boldsymbol{u}, 0)) \leq \epsilon\beta_2 \Psi(\boldsymbol{e}_x)\Phi(\tilde{z}) + \epsilon\gamma\Phi^2(\tilde{z}) \tag{20d}$$

$$\epsilon < \frac{\alpha_1\alpha_2}{\gamma\alpha_1 + \beta_1\beta_2} \tag{20e}$$

then the full-order closed-loop system is stable about the reference model in the sense of Lyapunov.

Proof: Define a composite candidate Lyapunov function

$$V = (1-d)V_s(\boldsymbol{e}_x, \tilde{\boldsymbol{\theta}}_s) + dV_f(\tilde{z}) \tag{21}$$

where $0 < d < 1$. Differentiate with respect to slow time t_s:

$$\acute{V} = (1-d)\acute{V}_s(\boldsymbol{e}_x, \tilde{\boldsymbol{\theta}}_s) + d\acute{V}_f(\tilde{z}) \tag{22}$$

Note that because t_s and t_f are all proportional by positive scalars, $\text{sign}(\acute{V}) = \text{sign}(\grave{V})$. In other words, proving stability in the slow time is equivalent to proving stability in the other timescales. Using the chain rule

$$\acute{V} = (1-d)\left[\frac{\partial V_s}{\partial \boldsymbol{e}_x}\acute{\boldsymbol{e}}_x + \frac{\partial V_s}{\partial \tilde{\boldsymbol{\theta}}_s}\acute{\tilde{\boldsymbol{\theta}}}_s\right] + d\left[\frac{\partial V_f}{\partial \tilde{z}}\acute{z}\right] \tag{23}$$

Substituting the definitions of the errors from Eqs. (8) and (10),

$$\acute{V} = (1-d)\left[\frac{\partial V_s}{\partial \boldsymbol{e}_x}(\acute{\boldsymbol{x}} - \acute{\boldsymbol{x}}_m) + \frac{\partial V_s}{\partial \tilde{\boldsymbol{\theta}}_s}\left(\acute{\hat{\boldsymbol{\theta}}}_s - \acute{\boldsymbol{\theta}}_s\right)\right] + d\left[\frac{\partial V_f}{\partial \tilde{z}}(\acute{z} - \acute{z}_0)\right] \tag{24}$$

Using $\epsilon(\acute{\cdot}) = (\grave{\cdot})$

$$\acute{V} = (1-d)\left[\frac{\partial V_s}{\partial \boldsymbol{e}_x}(\acute{\boldsymbol{x}} - \acute{\boldsymbol{x}}_m) + \frac{\partial V_s}{\partial \tilde{\boldsymbol{\theta}}_s}\left(\acute{\hat{\boldsymbol{\theta}}}_s - \acute{\boldsymbol{\theta}}_s\right)\right] + \frac{d}{\epsilon}\left[\frac{\partial V_f}{\partial \tilde{z}}(\grave{z} - \grave{z}_0)\right] \tag{25}$$

The manifold $z_0 = h(\boldsymbol{x}, \boldsymbol{u})$ is the trajectory the fast states system converges to as time goes to infinity. By definition of composite control, $u_f = 0$ when $z = z_0$. Therefore the manifold can be rewritten as $z_0 = h(\boldsymbol{x}, \boldsymbol{u}_s)$. Using the definitions given by conditions (A), (B), and (D) in Theorem 2 and (J) in Theorem 4,

$$\begin{aligned}\dot{V} = (1-d)\Bigg[&\frac{\partial V_s}{\partial \boldsymbol{e}_x}(f(\boldsymbol{x}, z, \boldsymbol{u}) - m(\boldsymbol{x}_m, \boldsymbol{r})) \\ &+ \frac{\partial V_s}{\partial \tilde{\boldsymbol{\theta}}_s}\Big(l(\boldsymbol{x}, \boldsymbol{x}_m) - \dot{q_s}(\boldsymbol{x}, t_s)\Big)\Bigg] \\ &+ \frac{d}{\epsilon}\Bigg[\frac{\partial V_f}{\partial \tilde{z}}\Big(g(\boldsymbol{x}, z, \boldsymbol{u}, \epsilon) - \dot{h}(\boldsymbol{x}, \boldsymbol{u}_s)\Big)\Bigg]\end{aligned} \tag{26}$$

Add and subtract $[(1-d)(\partial V_s/\partial \boldsymbol{e}_x) f(\boldsymbol{x}, z_0, \boldsymbol{u}_s) + (d/\epsilon)(\partial V_f/\partial \tilde{z})\, g(\boldsymbol{x}, z, \boldsymbol{u}, 0)]$

$$\begin{aligned}\dot{V} = (1-d)\Bigg[&\frac{\partial V_s}{\partial \boldsymbol{e}_x}(f(\boldsymbol{x}, z_0, \boldsymbol{u}_s) - m(\boldsymbol{x}_m, \boldsymbol{r})) + \frac{\partial V_s}{\partial \tilde{\boldsymbol{\theta}}_s}\Big(l(\boldsymbol{x}, \boldsymbol{x}_m) \\ &- \dot{q_s}(\boldsymbol{x}, t_s)\Big) + \frac{\partial V_s}{\partial \boldsymbol{e}_x}(f(\boldsymbol{x}, z, \boldsymbol{u}) - f(\boldsymbol{x}, z_0, \boldsymbol{u}_s))\Bigg] \\ &+ \frac{d}{\epsilon}\Bigg[\frac{\partial V_f}{\partial \tilde{z}}\Big(g(\boldsymbol{x}, z, \boldsymbol{u}, 0) - \dot{h}(\boldsymbol{x}, \boldsymbol{u}_s)\Big) \\ &+ \frac{\partial V_f}{\partial \tilde{z}}(g(\boldsymbol{x}, z, \boldsymbol{u}, \epsilon) - g(\boldsymbol{x}, z, \boldsymbol{u}, 0))\Bigg]\end{aligned} \tag{27}$$

Via the conditions in Eqs. (20a–20d),

$$\begin{aligned}\dot{V} \le (1-d)\big[&-\alpha_1 \Psi^2(\boldsymbol{e}_x) + \beta_1 \Psi(\boldsymbol{e}_x)\Phi(\tilde{z})\big] \\ &+ \frac{d}{\epsilon}\big[-\alpha_2 \Phi^2(\tilde{z}) + \epsilon\beta_2 \Psi(\boldsymbol{e}_x)\Phi(\tilde{z}) + \epsilon\gamma\Phi^2(\tilde{z})\big]\end{aligned} \tag{28}$$

Some algebra gives

$$\begin{aligned}\dot{V} \le -\big[\Psi(\boldsymbol{e}_x)^\top \;\; \Phi(\tilde{z})^\top\big]&\begin{bmatrix} (1-d)\alpha_1 & -\frac{1}{2}((1-d)\beta_1 + d\beta_2) \\ -\frac{1}{2}((1-d)\beta_1 + d\beta_2) & \frac{d}{\epsilon}\alpha_2 - d\gamma \end{bmatrix} \\ \times&\begin{bmatrix} \Psi(\boldsymbol{e}_x) \\ \Phi(\tilde{z}) \end{bmatrix}\end{aligned} \tag{29}$$

The full-order closed-loop system is asymptotically stable if the matrix in Eq. (29) is positive definite. Sylvester's criterion [31] says that this matrix is positive definite if and only if $\alpha_1 > 0$ (guaranteed by definition) and

$$0 < (1-d)\alpha_1\left(\frac{d}{\epsilon}\alpha_2 - d\gamma\right) - \frac{1}{4}((1-d)\beta_1 + d\beta_2)^2 \tag{30}$$

Solving for ϵ

$$\epsilon < \frac{\alpha_1\alpha_2}{\gamma\alpha_1 + \frac{1}{4d(1-d)}((1-d)\beta_1 + d\beta_2)^2} \tag{31}$$

d is any arbitrary real value between zero and one. An optimization can give us the value of d that allows the largest valid range for the timescale separation parameter. The solution to this optimization problem is given by [1] (p. 42). The upper limit on the valid range for the timescale separation parameter is

$$\epsilon^* = \frac{\alpha_1\alpha_2}{\gamma\alpha_1 + \beta_1\beta_2} \tag{32}$$

By the condition in Eq. (20e), $\epsilon < \epsilon^*$. Thus, by Lyapunov's second method, the system is stable about the reference model in the sense of Lyapunov. □

The conclusions of Theorem 4 are equivalent to Theorem 3 (Lyapunov stability). However, Theorem 4 offers a few unique benefits. First, Theorem 4 gives a bound on the timescale separation parameter. This gives a measure of the robustness of the control to timescale separation uncertainties. Second, the conditions of Theorem 4 are more practical. Note that the condition in Eq. (20b) is the same condition that is difficult to address in Theorems 2 and 3; namely, the manifold of the closed-loop model is an asymptotically stable equilibrium of the fast states. However, in the case of Theorem 4 there is a simple way to verify that this condition is met. A third benefit is that, in some cases, Barbalat's lemma [32] can be used to show convergence. The following corollary to Theorem 4 is also notable.

Corollary 3: Theorem 4 also applies to ROAC.

Proof: ROAC is equivalent to KAMS when the fast control is selected to be $u_f = 0$. Thus, Theorem 4 can be used to find a valid range for the timescale separation parameter of a system under ROAC. □

The benefits of Theorem 4 come with a cost. First, a Lyapunov function must be found such that the conditions are satisfied. Finding a Lyapunov function can be particularly challenging when consideration is given to the time rate of change of the manifold $\dot{h}(\boldsymbol{x}, \boldsymbol{u}_s)$ in the condition from Eq. (20b). This challenge is not unique to adaptive multiple-timescale control. Saberi and Khalil encountered this when proposing their nonadaptive solution. They proposed adding an additional condition constraining $(\partial V_f/\partial \tilde{z})(\partial h/\partial \boldsymbol{x}) f(\boldsymbol{x}, z, \boldsymbol{u})$. Sabiri and Khalil also considered systems with fast Lyapunov functions that are also dependent upon the slow states. These alterations could also be applied to adaptive systems. See Sabiri and Khalil's work for more details [30,33].

IV. Example

Adaptive control has a long history of application to aerospace systems. For example, adaptive control has been applied to an F-16 [34], an F/A-18A [35], and an uncrewed air system (UAS) [36]. Multiple-timescale control has also been applied to aerospace systems. For example, multiple-timescale control has been applied to a generic fixed-wing aircraft [37], an F-16A [6], and trajectory optimization [38]. For more examples, see [8]. However, relatively little research has addressed the effects of timescales on adaptive control for aerospace systems.

Consider the linearized second-order short-period longitudinal dynamics of a fixed-wing aircraft. The elevator actuator dynamics can also be represented as a second-order system [39,40]. In this paper, it is assumed that the elevator dynamics are significantly faster than the short-period dynamics. This system can be represented with the following set of equations:

$$\dot{\boldsymbol{x}} = A_x \boldsymbol{x} + B_x \Lambda \delta_e \tag{33a}$$

$$\epsilon \dot{z} = A_z z + B_z \delta_{e,c} \tag{33b}$$

The variables A_x, $A_z \in \mathbb{R}^{2\times 2}$ and B_x, $B_z \in \mathbb{R}^{2\times 1}$ are system parameters, with A_x being uncertain. The variable $\Lambda \in \mathbb{R}_+$ represents the control effectiveness of δ_e and is also uncertain. The state vectors $\boldsymbol{x}$ and z are defined as $\boldsymbol{x} \triangleq [\,\alpha \quad q\,]^T$ and $z \triangleq [\,\delta_e \quad \dot{\delta}_e\,]^T$. The variable q is the body-axis pitch rate and α is the angle of attack. The variable δ_e is the elevator deflection and $\delta_{e,c}$ is the commanded elevator deflection. The state and control variables are taken to be zero at trim. Finally, by definition, let the first column of A_z is equal to $-B_z$. This implies that the DC gain for the fast actuator dynamics is one and that $-A_z^{-1}B_z \triangleq [\,1 \quad 0\,]^T$. This is the full-order multiple-timescale system. Following the procedure in Sec. II, the reduced slow model is

$$\dot{\boldsymbol{x}} = A_x \boldsymbol{x} + B_x \Lambda \delta_e \tag{34a}$$

$$z_0 = [\,\delta_{e,c} \quad 0\,]^T \tag{34b}$$

The reduced fast model is

$$\dot{\tilde{\boldsymbol{x}}} = 0 \tag{35a}$$

$$\dot{\boldsymbol{z}} = A_z \boldsymbol{z} + B_z \delta_{e,c} \tag{35b}$$

The subsystems are now used to develop control laws. The control objective will be for the angle of attack α to track a reference model with a sinusoidal input.

A. Control Synthesis

In this section, a FOAC, a ROAC, and a KAMS adaptive controller are designed. The reference model is Eq. (7). This will be a second-order reference model for ROAC and KAMS, but a fourth-order reference model for FOAC (because FOAC considers the full-order system). For the sake of demonstration, a simple model reference adaptive control (MRAC) law is used within the frameworks of FOAC, ROAC, and KAMS. More details can be found in [41] (pp. 111–116).

1. Full-Order Adaptive Control

As described above, ϵ can be moved to the right side of Eq. (33b), and $\boldsymbol{x}$ and $\boldsymbol{z}$ can be concatenated into a single state vector. This yields the full-order block-matrix system

$$\begin{bmatrix} \dot{\boldsymbol{x}} \\ \dot{\boldsymbol{z}} \end{bmatrix} = \begin{bmatrix} A_x & [B_x \quad 0_{2\times 1}] \\ 0_{2\times 2} & A_z \frac{1}{\epsilon} \end{bmatrix} \begin{bmatrix} \boldsymbol{x} \\ \boldsymbol{z} \end{bmatrix} + \begin{bmatrix} 0_{2\times 1} \\ B_z \frac{1}{\epsilon} \end{bmatrix} \delta_{e,c} \tag{36}$$

The notation $0_{i\times j}$ indicates an $i \times j$-dimensional matrix of zeros. An adaptive controller can be selected from a wide class of adaptive algorithms for linear systems. In this case, traditional MRAC from [41] (pp. 111–116) is selected

$$\delta_{e,c} = \hat{K}_x \boldsymbol{x} + \hat{K}_z \boldsymbol{z} + \hat{K}_r r \tag{37a}$$

$$\begin{bmatrix} \dot{\hat{K}}_x & \dot{\hat{K}}_z \end{bmatrix}^T = -\Gamma_{xz} \begin{bmatrix} \boldsymbol{x} \\ \boldsymbol{z} \end{bmatrix} \begin{bmatrix} \boldsymbol{e}_x^T & \boldsymbol{e}_z^T \end{bmatrix} P_x \begin{bmatrix} 0_{2\times 1} \\ B_z \frac{1}{\epsilon} \end{bmatrix} \tag{37b}$$

$$\dot{\hat{K}}_r^T = -\Gamma_r r \begin{bmatrix} \boldsymbol{e}_x^T & \boldsymbol{e}_z^T \end{bmatrix} P_x \begin{bmatrix} 0_{2\times 1} \\ B_z \frac{1}{\epsilon} \end{bmatrix} \tag{37c}$$

where $\Gamma_{xz}, \Gamma_r \in \mathbb{R}^{4\times 4}$ are positive definite adaptation rate gain matrices that must be tuned. The variables $\hat{K}_x, \hat{K}_z \in \mathbb{R}^{1\times 2}$ and $\hat{K}_r \in \mathbb{R}$ are adapting control gains. The variable $P_x \in \mathbb{R}^{4\times 4}$ is also a positive definite matrix that is the solution to the Lyapunov equation $P_x A_m + A_m^T P_x = -Q_x$, where $Q_x \in \mathbb{R}^{4\times 4}$ is an arbitrary positive definite symmetric matrix. For the following simulation, Q_x is selected to be the identity matrix. Notably the timescale separation parameter is explicitly used in the adaptation laws. However, if it is unknown, then ϵ can be absorbed into the adaptation rate gains Γ_{xz} and Γ_r. By Theorem 1, the error $e_\alpha \triangleq \alpha - \alpha_m$ converges to zero and the system is bounded. Further, again by Theorem 1, all timescale separation parameters are valid for this system under FOAC.

2. Reduced-Order Adaptive Control

For ROAC, only the reduced slow subsystem is considered, and it is assumed that the fast states are always on their manifold (i.e., $\delta_e = \delta_{e,c}$). The reduced slow subsystem is therefore

$$\dot{\boldsymbol{x}} = A_x \boldsymbol{x} + B_x \Lambda \delta_{e,c} \tag{38}$$

An adaptive controller can be selected from a wide class of adaptive algorithms for linear systems. In this case, traditional MRAC from [41] (pp. 111–116) is used again:

$$\delta_{e,c} = \hat{K}_x \boldsymbol{x} + \hat{K}_r r \tag{39a}$$

$$\dot{\hat{K}}_x^T = -\Gamma_x \boldsymbol{x} \boldsymbol{e}_x^T P_x B_x \tag{39b}$$

$$\dot{\hat{K}}_r^T = -\Gamma_r r \boldsymbol{e}_x^T P_x B_x \tag{39c}$$

where $\Gamma_{xz}, \Gamma_r \in \mathbb{R}^{2\times 2}$ are positive definite adaptation rate gain matrices that must be tuned. To ensure that dimensions are consistent, P_x, $Q_x \in \mathbb{R}^{2\times 2}$, but these matrices serve the same role and are subject to the same constraints (e.g., positive definite) as they are with FOAC. By Theorem 2 and Corollary 2, there exists a set of timescale separation parameters such that the closed-loop tracking error e_α is bounded by a bound on the order of the timescale separation parameter. The set of valid timescale separation parameters for ROAC is discussed in the next section. However, the following Lyapunov function from [41] (pp. 111–116) is useful:

$$V_s = \boldsymbol{e}_x^T P_x \boldsymbol{e}_x + \text{trace}\left(\tilde{K}_x \Gamma_x^{-1} \tilde{K}_x^T\right) + \text{trace}\left(\tilde{K}_r \Gamma_r^{-1} \tilde{K}_r^T\right) \tag{40}$$

Again from [41] (pp. 111–116) it is known that

$$\dot{V}_s = -\boldsymbol{e}_x^T Q_x \boldsymbol{e}_x \tag{41}$$

$$\leq -\lambda_{\min}(Q_x) \|\boldsymbol{e}_x\|_2^2 \tag{42}$$

where $\lambda_{\min}(\cdot)$ is the smallest eigenvalue of $(\cdot)$.

3. KAMS

The adaptive controller designed in the previous section can be extended to be a KAMS controller by selecting the slow control $\delta_{e,c,s}$ to be the input from ROAC [Eq. (39)] and designing an additional controller for the fast states. A simple nonadapting linear control law is used for this purpose because there is no uncertainty in the reduced fast subsystem. The full-order control law can then be found using the definition of composite control $\delta_{e,c} = \delta_{e,c,s} + \delta_{e,c,f}$. Recall that $\boldsymbol{z}_0 \triangleq [\delta_{e,c,s} \quad 0]^T$. This is consistent with Eq. (34b) because by definition $\delta_{e,c,f} = 0$ when $\boldsymbol{z} = \boldsymbol{z}_0$. The reduced fast subsystem can be written as

$$\dot{\boldsymbol{z}} = A_z(\boldsymbol{z} - \boldsymbol{z}_0) + B_z \delta_{e,c,f} \tag{43}$$

because the first column of A_z is equal to $-B_z$. The fast control is selected to be $\delta_{e,c,f} = K_z(\boldsymbol{z} - \boldsymbol{z}_0)$. Note that K_z is a constant control gain that does not adapt. It must be tuned (this is made easier because A_z and B_z are not uncertain). Let K_z be chosen such that $A_z + B_z K_z$ is Hurwitz. In summary, the full-order control law is

$$\delta_{e,c} = \hat{K}_x \boldsymbol{x} + K_z(\boldsymbol{z} - \boldsymbol{z}_0) + \hat{K}_r r \tag{44a}$$

$$\dot{\hat{K}}_x^T = -\Gamma_x \boldsymbol{x} \boldsymbol{e}_x^T P_x B_x \tag{44b}$$

$$\dot{\hat{K}}_r^T = -\Gamma_r r \boldsymbol{e}_x^T P_x B_x \tag{44c}$$

Consider the following candidate Lyapunov function for the reduced fast system in Eq. (35):

$$V_f = \tilde{\boldsymbol{z}}^T P_z \tilde{\boldsymbol{z}} \tag{45}$$

The variable $P_z \in \mathbb{R}^{2\times 2}$ is the positive definite solution to the Lyapunov function $P_z(A_z + B_z K_z) + (A_z + B_z K_z)^T P_z = -Q_z$, where $Q_z \in \mathbb{R}^{2\times 2}$ is an arbitrary positive definite symmetric matrix. Differentiating gives

$$\dot{V}_f = -\tilde{\boldsymbol{z}}^T Q_z \tilde{\boldsymbol{z}} \tag{46}$$

$$\leq -\lambda_{\min}(Q_z) \|\tilde{\boldsymbol{z}}\|_2^2 \tag{47}$$

where it has been assumed that $\dot{\delta}_{e,c,s} = 0$. This is a good assumption because the slow input should vary on the slow timescale, not the fast timescale. However, it does decrease the accuracy of the bounds on

the timescale separation parameter. By Theorem 3 there exists a set of timescale separation parameters such that the closed-loop tracking error e_α is bounded by a bound on the order of the timescale separation parameter. A set of valid timescale separation parameters is found by applying Theorem 4. Let $\Psi(\boldsymbol{e}_x) = \|\boldsymbol{e}_x\|_2$ and let $\Phi(\tilde{\boldsymbol{z}}) = \|\tilde{\boldsymbol{z}}\|_2$.

Condition in Eq. (20a): By Eq. (42),

$$\alpha_1 = \lambda_{\min}(Q_x) \tag{48}$$

Condition in Eq. (20b): By Eq. (47),

$$\alpha_2 = \lambda_{\min}(Q_z) \tag{49}$$

Condition in Eq. (20c): Substituting Eq. (33a), Eq. (34a), and the partial of Eq. (40) into Eq. (20c)gives

$$2\boldsymbol{e}_x^T P_x\big[\big(A_x\boldsymbol{x} + B_x\Lambda\delta_e\big) - \big(A_x\boldsymbol{x} + B_x\Lambda\delta_{e,c}\big)\big] \le \beta_1\|\boldsymbol{e}_x\|_2\|\tilde{\boldsymbol{z}}\|_2 \tag{50}$$

Simplifying gives

$$2\boldsymbol{e}_x^T P_x B_x\Lambda[\delta_e - \delta_{e,c}] \le \beta_1\|\boldsymbol{e}_x\|_2\|\tilde{\boldsymbol{z}}\|_2 \tag{51}$$

Using $\delta_{e,c,f} = 0$ when $\boldsymbol{z} = \boldsymbol{z}_0$ and $\tilde{\boldsymbol{z}} = \boldsymbol{z} - \boldsymbol{z}_0$ and taking the two-norm gives

$$2\|\boldsymbol{e}_x\|_2\sigma_{\max}(P_x B_x\Lambda)\|\tilde{\boldsymbol{z}}\|_2 \le \beta_1\|\boldsymbol{e}_x\|_2\|\tilde{\boldsymbol{z}}\|_2 \tag{52}$$

where $\sigma_{\max}(\cdot)$ is the maximum singular value of $(\cdot)$. Therefore

$$\beta_1 = 2\sigma_{\max}(P_x B_x\Lambda) \tag{53}$$

Condition in Eq. (20d): Substituting Eq. (33b), Eq. (35b), and the partial of Eq. (45) Eq. (20d) gives

$$\begin{aligned} 2\tilde{\boldsymbol{z}}^T P_x\big[\big(A_z\boldsymbol{z} + B_z\delta_{e,c}\big) - \big(A_z\boldsymbol{z} + B_z\delta_{e,c}\big)\big] \\ \le \epsilon\beta_2\|\boldsymbol{e}_x\|_2\|\tilde{\boldsymbol{z}}\|_2 + \epsilon\gamma\|\tilde{\boldsymbol{z}}\|_2^2 \end{aligned} \tag{54}$$

Simplifying

$$0 \le \epsilon\beta_2\|\boldsymbol{e}_x\|_2\|\tilde{\boldsymbol{z}}\|_2 + \epsilon\gamma\|\tilde{\boldsymbol{z}}\|_2^2 \tag{55}$$

By definition, $\beta_2 \ne 0$ and $\gamma \ne 0$; therefore, let β_2 and γ be any arbitrary positive constant:

$$\beta_2 \in \mathbb{R}_+ \tag{56a}$$

$$\gamma \in \mathbb{R}_+ \tag{56b}$$

Condition in Eq. (20e): Finally, the bound on the timescale separation parameter is obtained from Eq. (20e). Substituting the results from Eqs. (48), (49), (53), and (56),

$$\epsilon < \frac{\lambda_{\min}(Q_x)\lambda_{\min}(Q_z)}{\gamma\lambda_{\min}(Q_x) + 2\sigma_{\max}(P_x B_x\Lambda)\beta_2} \tag{57}$$

All components of Eq. (57) are positive. Therefore, because β_2 and γ are arbitrary, the following conclusion can be drawn:

$$\forall 0 < \epsilon \ll 1 \quad \exists\gamma, \beta_2 \in \mathbb{R}_+ \quad \text{s.t.} \quad \epsilon < \frac{\lambda_{\min}(Q_x)\lambda_{\min}(Q_z)}{\gamma\lambda_{\min}(Q_x) + 2\sigma_{\max}(P_x B_x\Lambda)\beta_2} \tag{58}$$

By Theorem 4, the closed-loop system under KAMS is stable in the sense of Lyapunov for all values of the timescale separation parameter.

Now consider the range of valid timescale separation parameters for ROAC. KAMS is equivalent to ROAC when $K_z = 0$ (i.e., the fast control is always zero). Thus, there are two cases. First, if A_z is Hurwitz, then the Lyapunov equation $P_z(A_z + B_z K_z) + (A_z + B_z K_z)^T P_z = -Q_z$ holds when $K_z = 0$. However, if A_z is not Hurwitz, then there is no solution to the Lyapunov equation. Thus the boundedness of the closed-loop system cannot be guaranteed by Theorem 4. The manifold is not an asymptotically stable equilibrium of the fast states, so Theorem 2 is also invalid. Intuitively, ROAC cannot account for the neglected unstable fast dynamics.

4. Summary of Control Laws

The adaptive control equations for FOAC, ROAC, and KAMS are summarized and compared in Table 1. This allows the three methods to be directly compared. The most notable difference between FOAC and ROAC is that FOAC is a higher-order method. This makes sense because model reduction is an important step in ROAC and KAMS. Thus ROAC and KAMS have a second-order reference model, fewer adaption laws, and a simpler control law. Another notable difference is that ROAC cannot guarantee the stability of the system when A_z is non-Hurwitz (i.e., the fast dynamics are unstable). ROAC assumes that the fast dynamics are stable. Finally, Table 1 makes it clear that KAMS is an extension of ROAC. The only difference between the two is the addition of a fast control term in the control law. This one change allows the fast dynamics to be inherently unstable without destabilizing the closed-loop system. Thus KAMS is found to be simpler than FOAC and more capable than ROAC.

B. Numerical Results

The performance of FOAC, ROAC, and KAMS is compared for controlling the pitch dynamics of a Boeing 747-100/200. The Boeing 747-100/200 system from [42] (Appendix B Airplane J) is linearized about trim during an approach for landing (0 ft altitude, 131 knots true airspeed, 8.5° angle of attack, and a standard atmosphere). The system parameters for the actuator dynamics are not published, but the elevator rate saturates at $\dot{\delta}_e = 37^\circ\,\text{s}^{-1}$ [43]. Therefore, a second-order system with a natural frequency of 5.5 rad/s and a damping ratio

Table 1 Comparison of the three different control methodologies applied to Eq. (33)

Aspect of Method	FOAC	ROAC	KAMS
Model	4th order $\dot{\boldsymbol{x}}_m = A_m\boldsymbol{x}_m + B_m\boldsymbol{r}$	2nd order $\dot{\boldsymbol{x}}_m = A_m\boldsymbol{x}_m + B_m\boldsymbol{r}$	2nd order $\dot{\boldsymbol{x}}_m = A_m\boldsymbol{x}_m + B_m\boldsymbol{r}$
Adaptive law	$\begin{bmatrix}\dot{\hat{K}}_x^T \\ \dot{\hat{K}}_z^T\end{bmatrix} = -\Gamma_{xz}\begin{bmatrix}\boldsymbol{x} \\ \boldsymbol{z}\end{bmatrix}\begin{bmatrix}\boldsymbol{e}_x \\ \boldsymbol{e}_z\end{bmatrix}^T P_x\begin{bmatrix}0_{2\times1} \\ B_z(1/\epsilon)\end{bmatrix}$ $\dot{\hat{K}}_r^T = -\Gamma_r \quad r\quad \begin{bmatrix}\boldsymbol{e}_x \\ \boldsymbol{e}_z\end{bmatrix}^T P_x\begin{bmatrix}0_{2\times1} \\ B_z(1/\epsilon)\end{bmatrix}$	$\dot{\hat{K}}_x^T = -\Gamma_x\boldsymbol{x}\boldsymbol{e}_x^T P_x B_x$ $\dot{\hat{K}}_r^T = -\Gamma_r r\boldsymbol{e}_x^T P_x B_x$	$\dot{\hat{K}}_x^T = -\Gamma_x\boldsymbol{x}\boldsymbol{e}_x^T P_x B_x$ $\dot{\hat{K}}_r^T = -\Gamma_r r\boldsymbol{e}_x^T P_x B_x$
Control law	$\delta_{e,c} = \hat{K}_x\boldsymbol{x} + \hat{K}_z\boldsymbol{z} + \hat{K}_r r$	$\delta_{e,c} = \hat{K}_x\boldsymbol{x} + \hat{K}_r r$	$\delta_{e,c} = \hat{K}_x\boldsymbol{x} + K_z(\boldsymbol{z} - \boldsymbol{z}_0) + \hat{K}_r r$
Stability	Lyapunov sense stable	Lyapunov sense stable	Lyapunov sense stable
Valid ϵ	$\forall\epsilon \in (0, 1)$	A_z Hurwitz $\Rightarrow \forall\epsilon \in (0, 1)$	$\forall\epsilon \in (0, 1)$

of 0.707 is chosen so that the elevator has appropriate bandwidth but does not saturate. The adapting parameters are initialized at an estimate of the true value using the matching condition (see [41], pp. 111–116]). Uncertainty is added to the system parameters before calculating the true value. Uncertainty is created by sampling the estimated parameter values from a normal distribution with a mean of the true value and a standard deviation of 20% of the true value. The closed-loop poles for the slow state's reference model are selected to be real stable poles at -1 and -1.5. For FOAC, the reference model's fast poles are placed at -14 and -15. The adaptation rate gains Γ_x,

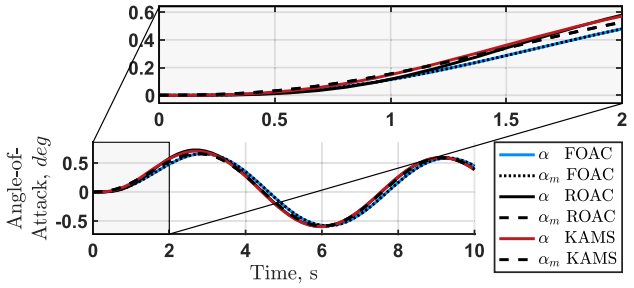

a) Time history of the angle-of-attack

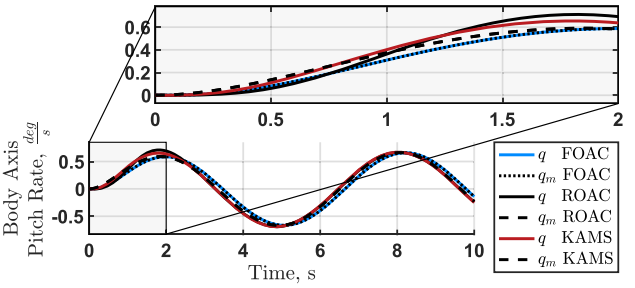

b) Time history of the body axis pitch rate

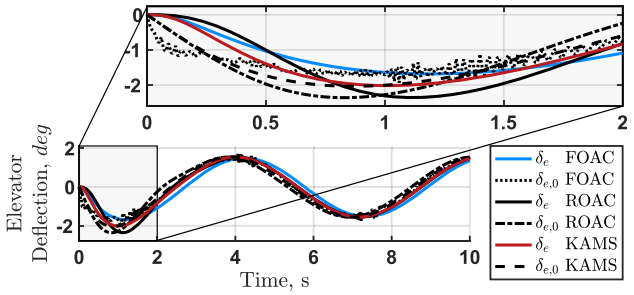

c) Time history of the elevator deflection

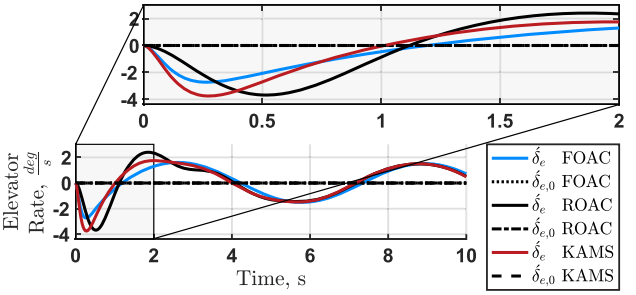

d) Time history of the elevator rate

Fig. 1 Time history of system states with high adaptation rate gains (10^5).

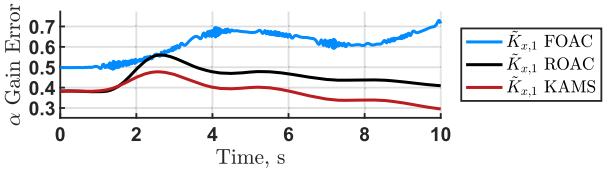

a) Time history of the angle-of-attack adapting gain

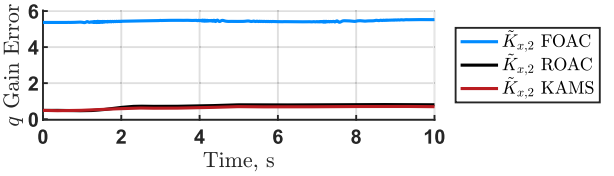

b) Time history of the body axis pitch rate adapting gain

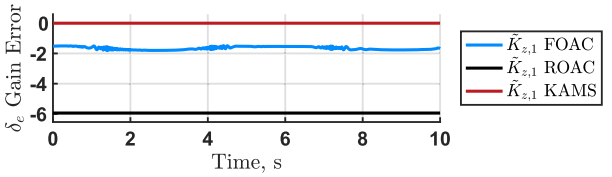

c) Time history of the elevator deflection adapting gain

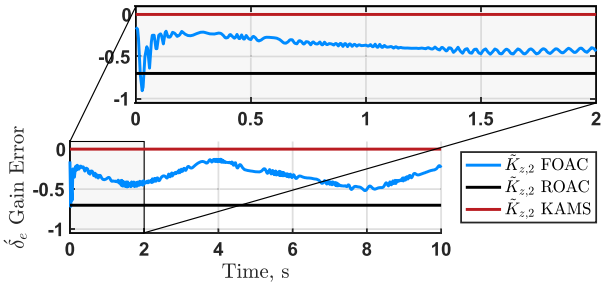

d) Time history of the elevator rate adapting gain

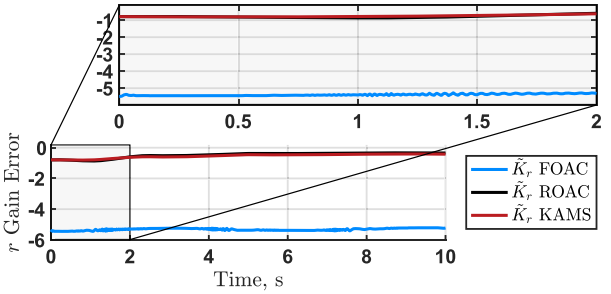

e) Time history of the reference model input adapting gain

Fig. 2 Time history of the control gains' error with high adaptation rate gains (10^5).

Γ_{xz}, and Γ_r are each tuned for optimal performance. The diagonal entries of each gain are found to be 10^5. The adaptation rate gains for each method (FOAC, ROAC, and KAMS) are kept equal to allow for direct comparison. The fast subsystem's control gain for KAMS (K_z) is found by using Ackermann's formula to place the poles of the fast subsystem at -14 and -15 (identical to FOAC). The system and reference models are initialized at trim. The reference model input is chosen to be $r = \sin(t_s)$ degrees angle of attack.

Figure 1a shows the time history of the angle of attack, Fig. 1b shows the time history of the body axis pitch rate, Fig. 1c shows the

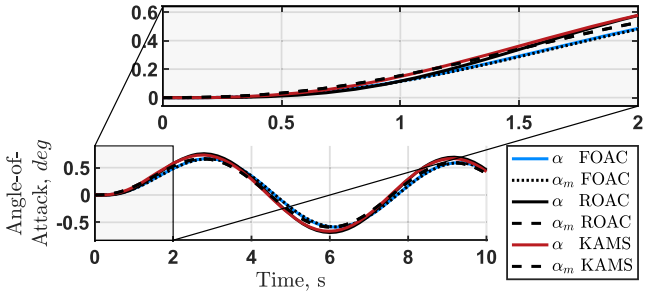

a) Time history of the angle-of-attack

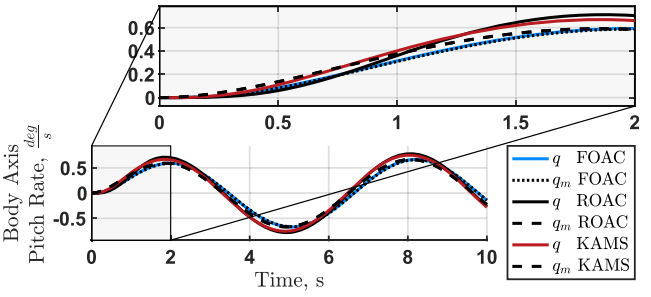

b) Time history of the body axis pitch rate

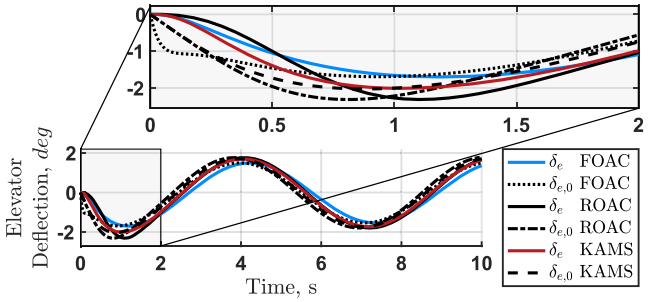

c) Time history of the elevator deflection

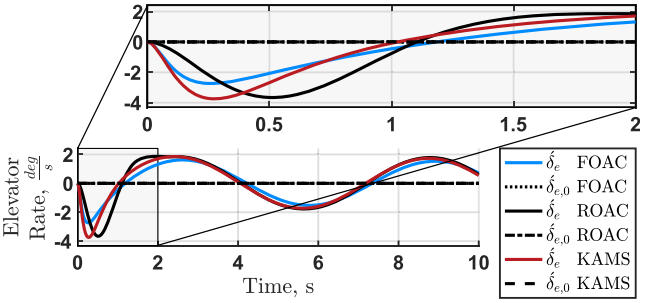

d) Time history of the elevator rate

Fig. 3 Time history of system states with reduced adaptation rate gains (1).

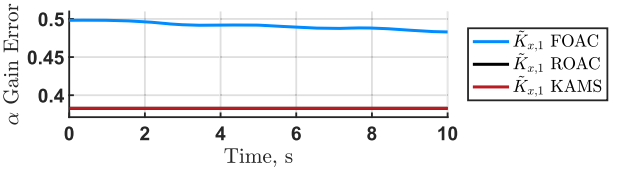

a) Time history of the angle-of-attack adapting gain

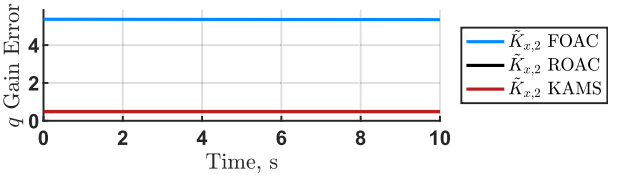

b) Time history of the body axis pitch rate adapting gain

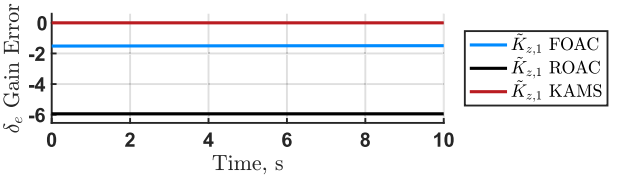

c) Time history of the elevator deflection adapting gain

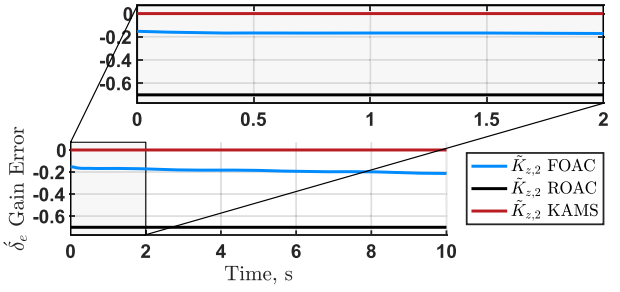

d) Time history of the elevator rate adapting gain

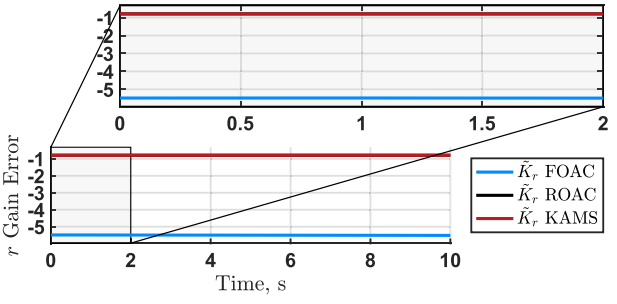

e) Time history of the reference model input adapting gain

Fig. 4 Time history of the control gains' error with reduced adaptation rate gains (1).

time history of the elevator deflection, and Fig. 1d shows the time history of the elevator rate. The adaptation gain time histories are shown in Fig. 2. All three multiple-timescale adaptive control methodologies—FOAC, ROAC, and KAMS—are shown for comparison, and all converge to the reference model. KAMS drives the elevator deflection to the manifold quicker and with less overshoot than the other methods because the fast control shapes the response of the fast states. Note that none of the control methods drives the elevator rate to the manifold. This is expected because the time-varying reference model makes this manifold physically impossible (the fast subsystem is underactuated). However, the control objective is slow state tracking, and so this is acceptable. Note that transient oscillations are visible in the elevator deflection rate under ROAC because it assumes that the fast dynamics are infinitely fast. FOAC demonstrates the best angle-of-attack tracking performance, but experiences high-frequency transient oscillations that are particularly evident in the time histories of the elevator deflection manifold and the adapting gains. This is a known and well-studied problem related to the system's timescales [44,45]. It is caused by high adaptation rate gains. In the previous example the adaptation rate gains for each controller are kept equal to allow for direct comparison. If the adaptation rate gains are reduced, the angle-of-attack tracking performance is degraded but the high-frequency oscillations under FOAC disappear. These results are visible in Figs. 3 and 4. The adaptation rate gains used for this second example are all identity. As a final test case, consider Figs. 5 and 6. These plots show what happens when the plant's fast dynamics are unstable. This effect is achieved by setting the damping ratio for the actuator dynamics equal

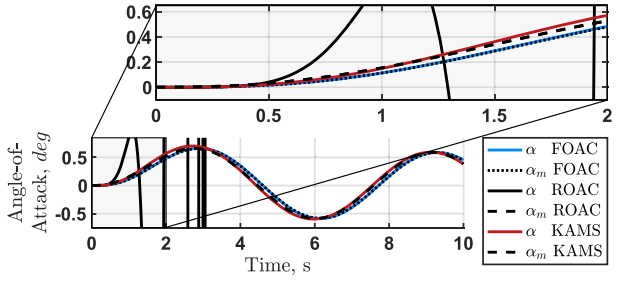

a) Time history of the angle-of-attack

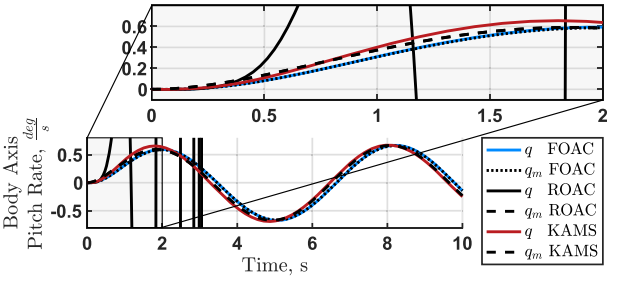

b) Time history of the body axis pitch rate

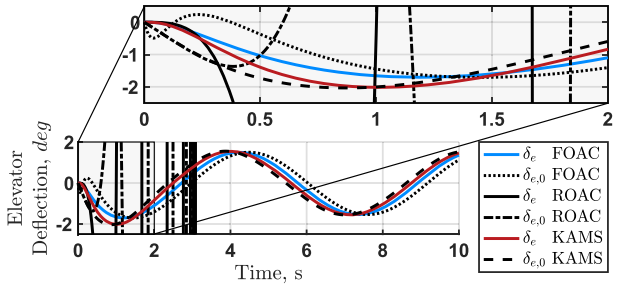

c) Time history of the elevator deflection

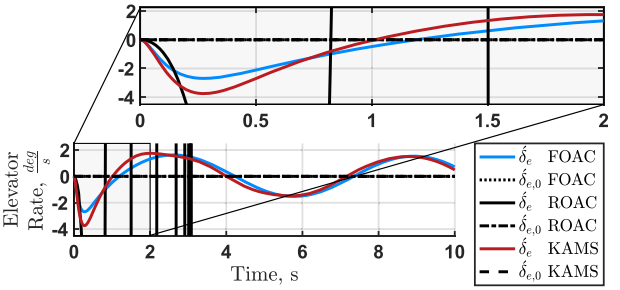

d) Time history of the elevator rate

Fig. 5 Time history of system states with unstable fast plant dynamics.

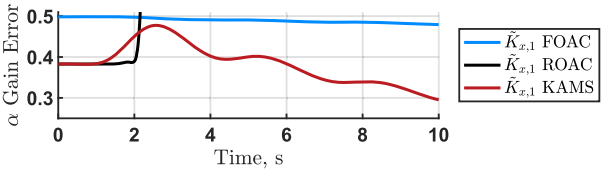

a) Time history of the angle-of-attack adapting gain

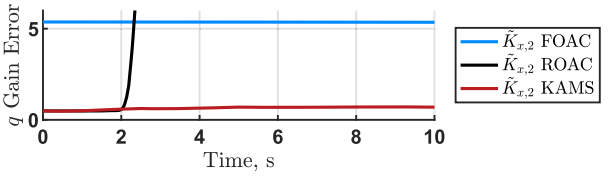

b) Time history of the body axis pitch rate adapting gain

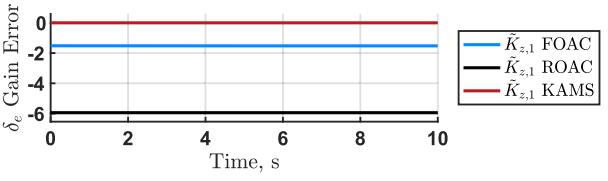

c) Time history of the elevator deflection adapting gain

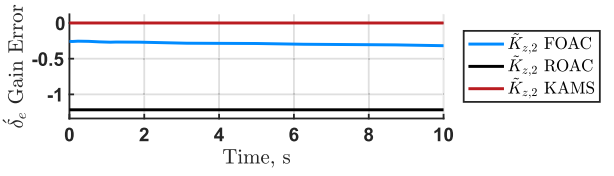

d) Time history of the elevator rate adapting gain

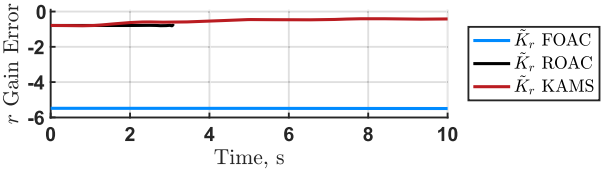

e) Time history of the reference model input adapting gain

Fig. 6 Time history of the control gains' error with unstable fast plant dynamics.

to −0.707. As predicted by the theoretical analysis in this paper, FOAC and KAMS can account for this, and their performance is relatively unaffected. On the other hand, the closed-loop system is dynamically unstable under ROAC. The adaptation rate gains for this final example are left at their best-case values. Low adaptation rate gains are used for ROAC in an attempt to decrease the rate of divergence for clarity in the plots. In summary, the diagonals of the adaptation rate gains are 1 for FOAC and ROAC, but 10^5 for KAMS.

V. Conclusions

This paper presented and developed three different adaptive control methodologies for multiple-timescale systems. FOAC uses traditional adaptive control on the full-order model. ROAC uses adaptive control on only one of the reduced-order models. KAMS uses adaptive control on both reduced-order models and then fuses the result. If uncertainties do not appear in one of the reduced-order models, then KAMS can also use a nonadaptive method on that reduced-order model. All three methodologies are shown to be Lyapunov sense stable under the theorems and associated conditions that are proven in this paper. An example with numerical results is given to demonstrate and compare all three methods. Based upon the theoretical and numerical results presented in the paper, the following conclusions are made.

Adaptive control can be sensitive to timescale effects. and so a method of adaptive control tailored specifically for multiple-timescale systems is needed. FOAC, ROAC, and KAMS are all valid adaptive multiple-timescale control methodologies. FOAC is the most straightforward because there is little to no additional work to reformat the plant, but it can be particularly sensitive to uncertainties in the timescale separation parameter and other timescale-related effects. ROAC allows the designer to take advantage of model reduction, which simplifies the control synthesis, but requires the discounted dynamics to be asymptotically stable. KAMS also takes advantage of model reduction but does not require the fast dynamics to be stable. Numerical results demonstrated that KAMS can be more robust to timescale effects than FOAC because it did not experience high-frequency oscillations at high adaptation rate gains. KAMS also demonstrated better fast state tracking performance than both of the other methods. This is because each reduced-order model is stabilized separately. For slow state tracking, KAMS performed slightly worse than FOAC, but slightly better than ROAC. KAMS tends to have a more complicated design process because two separate controllers must be designed. While all three methods are valid, KAMS is judged to provide the best balance between performance and robustness.

References

[1] Narang-Siddarth, A., and Valasek, J., *Nonlinear Multiple Time Scale Systems in Standard and Non-Standard Forms: Analysis & Control*, 1st ed., Soc. for Industrial and Applied Mathematics, Philadelphia, PA, 2014, Chaps. 2 & 3. https://doi.org/10.1137/1.9781611973341

[2] Tavasoli, A., Eghtesad, M., and Jafarian, H., "Two-Time Scale Control and Observer Design for Trajectory Tracking of Two Cooperating Robot Manipulators Moving a Flexible Beam," *Robotics and Autonomous Systems*, Vol. 57, No. 2, 2009, pp. 212–221. https://doi.org/10.1016/j.robot.2008.04.003

[3] Sauer, P. W., "Time-Scale Features and their Applications in Electric Power Systems Dynamic Modeling and Analysis," *American Control Conference*, Inst. of Electrical and Electronics Engineers, New York, 2011, pp. 4155–4159. https://doi.org/10.1109/ACC.2011.5991375

[4] Soner, H. M., "Singular Perturbations in Manufacturing," *Society for Industrial and Applied Mathematics Journal of Control and Optimization*, Vol. 31, No. 1, 1993, pp. 132–146. https://doi.org/10.1137/0331010

[5] Nguyen, N., Ishihara, A., Stepanyan, V., and Boskovic, J., "Optimal Control Modification for Robust Adaptation of Singularly Perturbed Systems with Slow Actuators," *Guidance, Navigation, and Control Conference and Exhibit*, AIAA Paper 2009-5615, 2009, pp. 1–21. https://doi.org/10.2514/6.2009-5615

[6] Saha, D., Valasek, J., Leshikar, C., and Reza, M. M., "Multiple-Timescale Nonlinear Control of Aircraft with Model Uncertainties," *Journal of Guidance, Control, and Dynamics*, Vol. 43, No. 3, 2020, pp. 536–552. https://doi.org/10.2514/1.G004303

[7] Ren, W., Jiang, B., and Yang, H., "Singular Perturbation-Based Fault-Tolerant Control of the Air-Breathing Hypersonic Vehicle," *Transactions on Mechatronics*, Vol. 24, No. 6, 2019, pp. 2562–2571. https://doi.org/10.1109/TMECH.2019.2946645

[8] Naidu, D. S., and Calise, A. J., "Singular Perturbations and Time Scales in Guidance and Control of Aerospace Systems: A Survey," *Journal of Guidance, Control, and Dynamics*, Vol. 24, No. 6, 2001, pp. 1057–1078. https://doi.org/10.2514/2.4830

[9] Hovakimyan, N., Lavretsky, E., and Sasane, A., "Dynamic Inversion for Nonaffine-in-Control Systems via Time-Scale Separation. Part I," *Journal of Dynamical and Control Systems*, Vol. 13, No. 4, 2007, pp. 451–465. https://doi.org/10.1007/s10883-007-9029-1

[10] Lavretsky, E., and Hovakimyan, N., "Adaptive Dynamic Inversion for Nonaffine-in-Control Uncertain Systems via Time-Scale Separation. Part II," *Journal of Dynamical and Control Systems*, Vol. 14, No. 1, 2008, pp. 33–41. https://doi.org/10.1007/s10883-007-9033-5

[11] Sun, T., Zhang, X., Yang, H., and Pan, Y., "Singular Perturbation-Based Saturated Adaptive Control for Underactuated Euler–Lagrange Systems," *International Society of Automation Transactions*, Vol. 119, Jan. 2022, pp. 74–80. https://doi.org/10.1016/j.isatra.2021.02.036

[12] Krishnamurthy, P., and Khorrami, F., "A Singular Perturbation Based Global Dynamic High Gain Scaling Control Design for Systems with Nonlinear Input Uncertainties," *Transactions on Automatic Control*, Vol. 58, No. 10, 2013, pp. 2686–2692. https://doi.org/10.1109/TAC.2013.2257968

[13] Asadi, M., and Khayatiyan, A., "Singular Perturbation Theory in Control of Nonlinear Systems with Uncertainties," *Iranian Conference on Electrical Engineering*, Inst. of Electrical and Electronics Engineers, New York, 2016, pp. 1908–1912. https://doi.org/10.1109/IranianCEE.2016.7585833

[14] Chakrabortty, A., and Arcak, M., "Time-Scale Separation Redesign for Stabilization and Performance Recovery for Uncertain Nonlinear Systems," *Automatica*, Vol. 45, No. 1, 2009, pp. 34–44. https://doi.org/10.1016/j.automatica.2008.06.004

[15] Rayguru, M. M., Ramalingam, B., and Elara, M. R., "A Singular Perturbation Based Adaptive Strategy for Bounded Controller Design in Feedback Linearizable Systems," *International Journal of Adaptive Control and Signal Processing*, Vol. 36, No. 2, 2021, pp. 264–281. https://doi.org/10.1002/acs.3360

[16] Yang, Y., Tang, L., Zou, W., and Ding, D.-W., "Robust Adaptive Control of Uncertain Nonlinear Systems with Unmodeled Dynamics Using Command Filter," *International Journal of Robust and Nonlinear Control*, Vol. 31, No. 16, 2021, pp. 7746–7784. https://doi.org/10.1002/rnc.5717

[17] Al-Radhawi, M. A., Sadeghi, M., and Sontag, E. D., "Long-Term Regulation of Prolonged Epidemic Outbreaks in Large Populations via Adaptive Control: A Singular Perturbation Approach," *Control System Letters*, Vol. 6, May 2021, pp. 578–583. https://doi.org/10.1109/LCSYS.2021.3083983

[18] Macchelli, A., Barchi, D., Marconi, L., and Bosi, G., "Robust Adaptive Control of a Hydraulic Press," *IFAC-PapersOnLine*, Vol. 53, No. 2, 2020, pp. 8790–8795. https://doi.org/10.1016/j.ifacol.2020.12.1384

[19] Saha, D., and Valasek, J., "Two-Time-Scale Slow and Fast State Tracking of an F-16 Using Slow and Fast Controls," *Guidance, Navigation, and Control Conference*, AIAA Paper 2017-1256, 2017. https://doi.org/10.2514/6.2017-1256

[20] Saha, D., Valasek, J., and Reza, M. M., "Two-Time-Scale Control of a Low-Order Nonlinear, Nonstandard System with Uncertain Dynamics," *Annual American Control Conference*, Inst. of Electrical and Electronics Engineers, New York, 2018, pp. 3720–3725. https://doi.org/10.23919/ACC.2018.8431384

[21] Saha, D., and Valasek, J., "Nonlinear Multiple-Time-Scale Attitude Control of a Rigid Spacecraft with Uncertain Inertias," *SciTech Forum*, AIAA Paper 2019-0932, 2019. https://doi.org/10.2514/6.2019-0932

[22] Ioannou, P. A., and Kokotovic, P., "Decentralized Adaptive Control of Interconnected Systems with Reduced-Order Models," *Automatica*, Vol. 21, No. 4, 1985, pp. 401–412. https://doi.org/10.1016/0005-1098(85)90076-7

[23] Vasil'eva, A. B., "Asymptotic Behaviour of Solutions to Certain Problems Involving Nonlinear Differential Equations Containing a Small Parameter Multiplying the Highest Derivatives," *Uspekhi Matematicheskikh Nauk*, Vol. 18, No. 3, 1963, pp. 15–86, http://www.mathnet.ru/php/archive.phtml?wshow=paper&jrnid=rm&paperid=6350&option_lang=eng.

[24] Tikhonov, A. N., "On the Dependence of the Solutions of Differential Equations on a Small Parameter," *Matematicheskii Sbornik Novaya Seriya*, Vol. 64, No. 2, 1948, pp. 193–204, http://www.mathnet.ru/php/archive.phtml?wshow=paper&jrnid=sm&paperid=6075&option_lang=eng.

[25] Khalil, H. K., *Nonlinear Systems*, 3rd ed., Prentice–Hall, Upper Saddle River, NJ, 2002, p. 361.

[26] Ioannou, P. A., and Sun, J., *Robust Adaptive Control*, Prentice–Hall, Upper Saddle River, NJ, 1996, pp. 110–111, 352–353.

[27] Gruenwald, B. C., Yucelen, T., and Muse, J. A., "Model Reference Adaptive Control in the Presence of Actuator Dynamics with Applications to the Input Time-Delay Problem," *Guidance, Navigation, and Control Conference*, AIAA Paper 2017-1491, 2017. https://doi.org/10.2514/6.2017-1491

[28] Hussain, H. S., "Robust Adaptive Control in the Presence of Unmodeled Dynamics," Ph.D. Thesis, Massachusetts Inst. of Technology, Cambridge, MA, 2017. 1721.1/111744

[29] Balas, M. J., "Feedback Control of Flexible Systems," *Transactions on Automatic Control*, Vol. 23, No. 4, 1978, pp. 673–679. https://doi.org/10.1109/TAC.1978.1101798

[30] Saberi, A., and Khalil, H., "Stabilization and Regulation of Nonlinear Singularly Perturbed Systems–Composite Control," *Transactions on Automatic Control*, Vol. 30, No. 8, 1985, pp. 739–747. https://doi.org/10.1109/TAC.1985.1104064

[31] Gilbert, G. T., "Positive Definite Matrices and Sylvester's Criterion," *American Mathematical Monthly*, Vol. 98, No. 1, 1991, pp. 44–46. https://doi.org/10.1080/00029890.1991.11995702

[32] Slotine, J.-J. E., and Li, W., *Applied Nonlinear Control*, Prentice–Hall, Upper Saddle River, NJ, 1991, pp. 122–126.

[33] Saberi, A., and Khalil, H., "Quadratic-Type Lyapunov Functions for Singularly Perturbed Systems," *Transactions on Automatic Control*, Vol. 29, No. 6, 1984, pp. 542–550. https://doi.org/10.1109/TAC.1984.1103586

[34] Tandale, M. D., and Valasek, J., "Fault-Tolerant Structured Adaptive Model Inversion Control," *Journal of Guidance, Control, and Dynamics*, Vol. 29, No. 3, 2006, pp. 635–642. https://doi.org/10.2514/1.15244

[35] Narang-Siddarth, A., and Valasek, J., "Kinetic State Tracking for a Class of Singularly Perturbed Systems," *Journal of Guidance, Control, and Dynamics*, Vol. 34, No. 3, 2011, pp. 734–749. https://doi.org/10.2514/1.52127

[36] Chowdhary, G., Johnson, E. N., Chandramohan, R., Kimbrell, M. S., and Calise, A., "Guidance and Control of Airplanes Under Actuator Failures and Severe Structural Damage," *Journal of Guidance, Control, and Dynamics*, Vol. 36, No. 4, 2013, pp. 1093–1104. https://doi.org/10.2514/1.58028

[37] Khalil, H. K., and Chen, F.-C., "Two-Time-Scale Longitudinal Control of Airplanes Using Singular Perturbation," *Journal of Guidance, Control, and Dynamics*, Vol. 13, No. 6, 1990, pp. 952–960. https://doi.org/10.2514/3.20566

[38] Ardema, M. D., and Rajan, N., "Separation of Time Scales in Aircraft Trajectory Optimization," *Journal of Guidance, Control, and Dynamics*, Vol. 8, No. 2, 1985, pp. 275–278. https://doi.org/10.2514/3.19972

[39] Ahmad, H., Young, T. M., Toal, D., and Omerdic, E., "Control Allocation with Actuator Dynamics for Aircraft Flight Controls," *Aviation Technology, Integration, and Operations Conference*, AIAA Paper 2007-7828, 2007. https://doi.org/10.2514/6.2007-7828

[40] Wagner, D., Henrion, D., and Hromčík, M., "Measures and LMIs for Validation of an Aircraft with MRAC and Uncertain Actuator Dynamics," *SciTech Forum*, AIAA Paper 2021-0531, 2021. https://doi.org/10.2514/6.2021-0531

[41] Nguyen, N. T., *Model-Reference Adaptive Control A Primer*, Advanced Textbooks in Control and Signal Processing, Springer, Berlin, 2018, pp. 111–116. https://doi.org/10.1007/978-3-319-56393-0

[42] Roskam, J., *Airplane Flight Dynamics and Automatic Flight Controls*, Vol. 1, Design, Analysis, and Research Corp., Lawrence, KS, 1995, Appendix B.

[43] Hanke, C. R., and Nordwall, D. R., "The Simulation of a Jumbo Jet Transport Aircraft Voume II: Modeling Data," Boeing Company for NASA, 1970, https://ntrs.nasa.gov/citations/19730001300.

[44] Gibson, T. E., Annaswamy, A. M., and Lavretsky, E., "Adaptive Systems with Closed–loop Reference Models, Part I: Transient Performance," *American Control Conference*, Inst. of Electrical and Electronics Engineers, New York, 2013, pp. 3376–3383. https://doi.org/10.1109/ACC.2013.6580353

[45] Yucelen, T., Torre, G. D. L., and Johnson, E. N., "Improving Transient Performance of Adaptive Control Architectures Using Frequency-Limited System Error Dynamics," *International Journal of Control*, Vol. 87, No. 11, 2014, pp. 2383–2379. https://doi.org/10.1080/00207179.2014.922702